environmental microbiology reports

Environmental Microbiology Reports (2021) **13**(2), 159–168 doi:10.1111/1758-2229.12919

Brief Report

Post-transcriptional deregulation of the *tisB/istR-1* toxin–antitoxin system promotes SOS-independent persister formation in *Escherichia coli*

Daniel Edelmann,[1] Markus Oberpaul,[3] Till F. Schäberle[2,3,4] and Bork A. Berghoff[1*]

[1]*Institute for Microbiology and Molecular Biology, Justus Liebig University Giessen, Giessen, 35392, Germany.*
[2]*Institute for Insect Biotechnology, Justus Liebig University Giessen, Giessen, 35392, Germany.*
[3]*Fraunhofer Institute for Molecular Biology and Applied Ecology (IME), Branch for Bioresources, Giessen, 35392, Germany.*
[4]*German Centre for Infection Research (DZIF), Partner Site Giessen-Marburg-Langen, Giessen, 35392, Germany.*

Summary

Bacterial dormancy is a valuable strategy to endure unfavourable conditions. The term 'persister' has been coined for cells that tolerate antibiotic treatments due to reduced cellular activity. The type I toxin–antitoxin system *tisB/istR-1* is linked to persistence in *Escherichia coli*, because toxin TisB depolarizes the inner membrane and causes ATP depletion. Transcription of *tisB* is induced upon activation of the SOS response by DNA-damaging drugs. However, translation is repressed both by a 5′ structure within the *tisB* mRNA and by RNA antitoxin IstR-1. This tight regulation limits TisB production to SOS conditions. Deletion of both regulatory RNA elements produced a 'high persistence' mutant, which was previously assumed to depend on stochastic SOS induction and concomitant TisB production. Here, we demonstrate that the mutant generates a subpopulation of growth-retarded cells during late stationary phase, likely due to SOS-independent TisB accumulation. Cell sorting experiments revealed that the stationary phase–derived subpopulation contains most of the persister cells. Collectively our data show that deletion of the regulatory RNA elements uncouples the persister formation process from the intended stress situation and enables the formation of TisB-dependent persisters in an SOS-independent manner.

Received 3 September, 2020; accepted 11 December, 2020. *For correspondence. E-mail bork.a.berghoff@mikro.bio.uni-giessen.de; Tel. +49 641 99 35558; Fax +49 641 99 35549.

Introduction

Bacteria have evolved so-called bet-hedging strategies to survive in fluctuating environments: some cells undergo a phenotypic change, which is commonly associated with the cost of strong growth retardation. While the majority of cells continue growing and contribute to the expansion of the population, the growth-retarded subpopulation is highly tolerant to multiple stress factors and ensures survival on the population level in case of fatal situations (Kussell and Leibler, 2005; Veening *et al*., 2008; Ackermann, 2015). A prominent example for a successful bet-hedging strategy is the formation of persister cells (Balaban *et al*., 2004; Harms *et al*., 2016; Van den Bergh *et al*., 2017). Persister cells were discovered in the 1940s, as they survived penicillin treatments (Hobby *et al*., 1942; Bigger, 1944). In fact, a hallmark of persister cells is their ability to tolerate high concentrations of many different antibiotics and to re-establish growing populations upon treatment termination. Therefore, they are associated with therapeutic failure and infection relapse (Lewis, 2010).

Spontaneous persister formation as a bet-hedging strategy is not the prevailing mode of persister formation. In many cases, persistence is triggered by stress and other environmental stimuli (Balaban *et al*., 2019; Kaldalu *et al*., 2020). For example, alarmone (p)ppGpp is produced in response to different stresses and in turn triggers persistence (Korch *et al*., 2003), which can be explained by (p)ppGpp-dependent ribosome dimerization (Song and Wood, 2020). Further environmental factors that trigger persistence include bacteriostatic agents (Kwan *et al*., 2013), low magnesium levels (Pontes and Groisman, 2019), host immune cells (Helaine *et al*., 2014) and DNA damage (Dörr *et al*., 2009). In laboratory cultures, persister levels typically reach a

maximum during the stationary phase (Keren *et al*., 2004; Harms *et al*., 2017), because persister formation is triggered by starvation. This type of persistence has been termed 'stationary-phase-induced persistence' (Balaban *et al*., 2019). Depending on culturing conditions, these stationary-phase persisters can 'contaminate' exponentially growing cultures, which has to be considered with caution when studying persistence in exponential phase (Balaban *et al*., 2004; Harms *et al*., 2017).

Studying the persister state is often complicated by the small size of persister fractions in culture samples. Large fractions of model persisters have been generated, e.g. by controllable expression of bacterial toxins or treatment with bacteriostatic agents (Kwan *et al*., 2013; Mok *et al*., 2015; Kim *et al*., 2018a; Kim *et al*., 2018b). Alternatively, mutants with an increased persister fraction, also called 'high persistence' (*hip*) mutants, have been employed as valuable systems for persister research. For example, kinase HipA is the toxin moiety from the type II toxin–antitoxin (TA) system HipAB (Black *et al*., 1991, 1994), and the high persistence *hipA7* mutant (Moyed and Bertrand, 1983) was regularly used to study persistence in *Escherichia coli* (Korch *et al*., 2003; Balaban *et al*., 2004; Keren *et al*., 2004). However, since HipA7 is non-toxic and has a different kinase activity compared with wild-type HipA (Korch *et al*., 2003; Semanjski *et al*., 2018), it remains doubtful whether the enriched persister fraction in *hipA7* cultures is evidence for toxin-mediated persistence in wild-type cultures.

In case of type II TA systems, there is an ongoing controversy concerning the direct link between toxins and persistence (Kim and Wood, 2016; Goormaghtigh *et al*., 2018). By contrast, toxins from type I TA systems are potential persistence factors due to their ability to affect membrane potential and intracellular ATP levels (Dörr *et al*., 2010; Gurnev *et al*., 2012; Verstraeten *et al*., 2015; Berghoff *et al*., 2017; Wilmaerts *et al*., 2018). In type I TA systems, the antitoxin is an RNA that prevents toxin production on the post-transcriptional level via sequestration of the toxin mRNA. Moreover, primary toxin mRNAs are translationally inert due to secondary structures that preclude ribosome binding (Berghoff and Wagner, 2019; Masachis and Darfeuille, 2018). A well-studied type I TA system is *tisB*/*istR-1* in *E. coli*. Toxin gene *tisB* is induced upon DNA damage as part of the SOS response, and transcription clearly depends on the SOS master regulator, LexA (Fernandez De Henestrosa *et al*., 2000; Vogel *et al*., 2004). Importantly, *tisB* is linked to persistence, since deletion of *tisB* reduces persister levels ~10-fold under DNA-damage conditions (Dörr *et al*., 2010; Berghoff *et al*., 2017). The primary *tisB* transcript (+1 mRNA) is translationally inert due to a secondary structure within the 5′ untranslated region (Darfeuille *et al*., 2007). A processing step removes the first 41 nucleotides from the 5′ end, which produces the translationally active +42 mRNA. Under growth-promoting conditions, antitoxin IstR-1 is in excess and efficiently sequesters the +42 mRNA, which triggers its degradation (Vogel *et al*., 2004; Darfeuille *et al*., 2007). However, when +42 mRNA accumulates upon DNA damage, TisB production is favoured and contributes to drug-induced persistence (Dörr *et al*., 2010; Berghoff *et al*., 2017; Balaban *et al*., 2019). Deletion of the two regulatory RNA elements (5′ structure in *tisB* +1 mRNA and antitoxin IstR-1) produced a mutant (Δ1-41 Δ*istR*) with a *hip* phenotype, which was tentatively explained by stochastic SOS induction and production of toxin TisB throughout growth (Berghoff *et al*., 2017). TisB is a small hydrophobic protein that is located in the cytoplasmic membrane and causes breakdown of the proton motive force, which leads to membrane depolarization, ATP depletion and subsequent persister formation (Unoson and Wagner, 2008; Gurnev *et al*., 2012; Berghoff *et al*., 2017).

In the current study, we demonstrate that the *hip* phenotype of the deregulated mutant Δ1-41 Δ*istR* is based on LexA-independent *tisB* expression. Hence, post-trans criptional deregulation of the *tisB* gene has uncoupled the persister formation process from SOS induction.

Results and discussion

Persisters in the deregulated mutant originate from stationary phase

In this study, *E. coli* K-12 wild-type MG1655 and corresponding mutant strains were grown to late stationary phase, which was defined as 20 h after inoculating single colonies into liquid LB medium. Upon dilution of late stationary-phase cultures into fresh medium, lag phase was extended by approximately 60 min in Δ1-41 Δ*istR* (from now on ΔΔ) compared with wild-type cultures, as inferred from optical density (Fig. 1A) and validated by total cell counts (Supporting Information Fig. Fig. S1). Ectopic overexpression of antitoxin IstR-1 restored the wild-type phenotype, verifying that TisB production was responsible for the observed growth delay (Fig. 1A). Doubling times during exponential growth were not statistically different between strains (31.1 ± 0.9 min for wild type, 32.2 ± 0.5 min for ΔΔ and 31.5 ± 0.2 for ΔΔ pIstR-1), demonstrating that the TisB-dependent effect was limited to initial growth resumption. Determination of single-cell lag times revealed that the median lag time of ΔΔ cells was approximately 30 min longer (Supporting Information Figs S2A and S2B). These results indicated that other factors contributed to the extended lag phase in bulk experiments.

We applied light scattering in flow cytometry experiments to analyse cells at different growth stages.

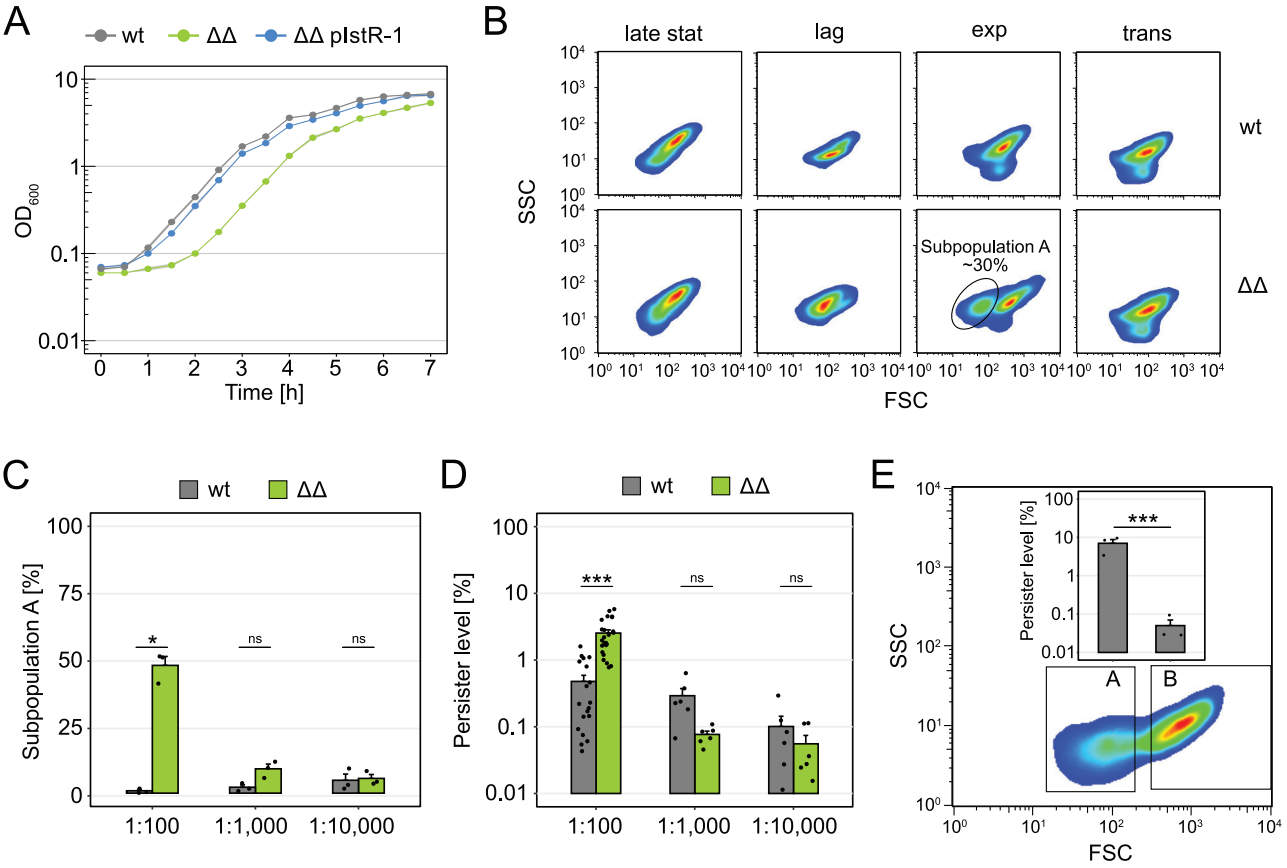

Fig. 1. Persisters of mutant Δ1-41 Δ*istR* originate from late stationary phase. A. Growth curves (OD_{600}) of late stationary-phase cultures diluted 1:100 into fresh LB medium. Lines indicate the mean and grey ribbons indicate the standard error of the mean (SEM; $n = 3$). In most instances, SEMs are too small to be visible. B. Flow cytometry analysis at various growth stages. Events were depicted as heat maps in scatter plots (FSC: forward scatter; SSC: side scatter). A representative experiment of biological triplicates is shown. The circle indicates the location of subpopulation A, which is absent in wt cultures. Percentage of subpopulation A is relative to all cells ($n > 3$). (late stat: late stationary phase, 20 h after inoculation; lag: 30 min after 100-fold dilution into fresh medium; exp: exponential phase, OD_{600} of 0.4; trans: transition phase, OD_{600} of 2.0). C. The size of subpopulation A was determined by flow cytometry at an OD_{600} of 0.4 after different dilutions of late stationary-phase cultures. Bars represent the mean (±SEM; $n = 3$). Black points represent the results of individual biological experiments. Original data can be found in Supporting Information Fig. S6. D. Influence of dilution on persister levels. Late stationary-phase cultures were diluted into fresh LB medium and grown until an OD_{600} of 0.4 was reached. Colony counts were determined before and after 6 h of CF treatment (1 μg ml^{-1}; 100× MIC) to calculate persister levels. Bars represent the mean (±SEM; $n \geq 6$). Black points indicate the results of individual biological experiments. E. Gates for cell sorting are depicted. 500 000 events were sorted for subpopulations A and subpopulation B of the ΔΔ mutant. Samples for sorting were from exponential phase (OD_{600} of 0.4). Colony counts were determined in sorted subpopulations before and after 6 h of CF treatment (1 μg ml^{-1}; 100× MIC) to calculate persister levels. Bars represent the mean (±SEM; $n = 3$). Black points indicate the results of individual biological experiments. If applicable, pairwise *t*-tests were performed (***$P < 0.001$, *$P < 0.05$, ns: not significant). (wt: wild type MG1655; ΔΔ: Δ1-41 Δ*istR*; pIstR-1: IstR-1 overexpression plasmid).

Population profiles of wild-type and ΔΔ cultures were very similar in late stationary phase (Fig. 1B). However, in lag phase (30 min after dilution), slight differences occurred, and in exponential phase, population profiles were quite different. In ΔΔ cultures, only two-thirds of the population resembled the profile of exponentially growing wild-type cells. Approximately one-third was more similar to stationary-phase cells with regard to cell length as judged from the forward scatter (subpopulation A; Fig. 1B). Under our experimental conditions, we did never observe such a subpopulation in exponential wild-type cultures. It is known that *E. coli* cells shrink during stationary phase and adopt a coccoid morphology (Nyström, 2004). Indeed, light microscopy validated that ΔΔ cultures retained a subpopulation of cells with a length similar to stationary-phase cells (Supporting Information Fig. S3). This subpopulation likely represented cells that had not fully proceeded to growth resumption. Upon continuous cultivation, the subpopulation disappeared, and wild-type and ΔΔ cultures were finally indistinguishable in transition phase (Fig. 1B). Accordingly, the *hip* phenotype of the ΔΔ mutant was only evident during lag and exponential phase, but persister levels were comparable to wild type in transition phase

(Supporting Information Fig. S4A). For persister assays, cultures were treated with the DNA-damaging fluoroquinolone ciprofloxacin (CF) at a concentration of 100× MIC (minimum inhibitory concentration) for 6 h. Biphasic kill curves revealed the existence of persisters and demonstrated that the 6-h time point was a good representation of persister levels in both wild-type and ΔΔ cultures (Supporting Information Fig. S5A). In contrast to recent reports (Harms *et al*., 2017), we did not observe major differences between CF at 100× and 1000× MIC (Supporting Information Fig. S5B). We, therefore, used CF at 100× MIC for 6 h in all subsequent persister assays.

To validate that subpopulation A in ΔΔ cultures originated from stationary-phase cells, the number of inoculated cells from stationary-phase cultures was reduced to allow more cells to resume growth until a defined optical density was reached. More precisely, late stationary-phase cultures were diluted 1:100, 1:1000 or 1:10 000, and grown until an optical density at 600 nm (OD_{600}) of 0.4 (exponential phase) was reached. As expected, the size of subpopulation A decreased with the number of inoculated cells (Fig. 1C and Supporting Information Fig. S6). We assume that subpopulation A mainly contains non-growing cells and that extended cultivation enables growth resumption of these cells, but this needs further investigation. The observed features were reminiscent of stationary-phase persisters (Balaban *et al*., 2004), and we speculated that the *hip* phenotype in ΔΔ cultures was linked to the existence of subpopulation A. The dilution experiment was repeated, and cultures were treated directly with CF when an OD_{600} of 0.4 (exponential phase) was reached. In wild-type cultures, persister levels decreased with the number of inoculated cells, indicating the elimination of stationary-phase persisters (Balaban *et al*., 2004; Keren *et al*., 2004). Likewise, the *hip* phenotype of the ΔΔ mutant was completely lost upon strong dilution (Fig. 1D). To directly prove that subpopulation A has an enriched persister fraction, subpopulations A and B were sorted based on their specific light scattering characteristics in flow cytometry experiments (Fig. 1E). Both subpopulations were subsequently treated with CF. As expected, subpopulation A contained approximately 200-fold more persisters than subpopulation B (Fig. 1E).

Live–dead cell viability assay was applied to reveal cells with damaged membranes, as indicated by strong staining with propidium iodide in relation to SYTO 9 stain (Supporting Information Fig. S7A). Subpopulation A had an increased proportion of cells with a damaged membrane in comparison to subpopulation B (7.3% versus 1.9% respectively). However, for 92.7% of cells staining did not indicate major damage (Supporting Information Fig. S7B). We conclude that subpopulation A mainly contains cells with an intact membrane, many of which are persisters that originate from stationary phase.

Deregulation of tisB *reduces cell viability in late stationary phase*

Bacterial cultures exhibit increasing levels of persister cells during stationary phase due to triggered formation of stationary-phase (type I) persisters (Balaban *et al*., 2004; Keren *et al*., 2004; Jõers *et al*., 2010; Harms *et al*., 2017). However, persister levels in ΔΔ cultures were surprisingly low during late stationary phase (Supporting Information Fig. S4A), which is counterintuitive, since we have shown that the *hip* phenotype of the mutant during exponential phase originates from stationary-phase cells (Fig. 1). Interestingly, the ΔΔ mutant formed approximately 16-fold less colonies than the wild type when late stationary-phase cultures were plated on regular LB agar plates (Fig. 2A), even though total cell counts were comparable (Fig. 2B). We recently reported a plating defect for the ΔΔ mutant during exponential phase when the oxidative stress regulator gene *soxS* was deleted. The plating defect was counteracted by addition of thiourea to LB agar plates, which is a scavenger of reactive oxygen species (Edelmann and Berghoff, 2019). Thiourea and the hydrogen peroxide-degrading enzyme catalase counteract the plating defect of a *Shewanella oneidensis* strain deleted for *oxyR*, encoding another important oxidative stress regulator (Shi *et al*., 2015), and the same was observed here for an *E. coli oxyR* deletion strain (Supporting Information Fig. S8). However, neither thiourea nor catalase in LB agar plates improved culturability of ΔΔ cultures (Supporting Information Fig. S8), indicating that a plating defect cannot account for the observed reduction in colony counts (Fig. 2A). Alternatively, ΔΔ cultures might have a reduced number of viable cells. Indeed, when late stationary-phase cultures were serially diluted and cultivated in liquid LB medium, an at least fourfold reduction in viability was observed (Supporting Information Fig. S2C). Together, these data clearly suggested that ΔΔ cultures contained more non-viable cells than wild-type cultures. The increased fraction of non-viable cells likely contributed to the extended lag phase of the ΔΔ mutant (Fig. 1A). Live–dead cell viability assay revealed that most ΔΔ cells had an intact membrane (96.4%; Supporting Information Fig. S7C), which is in agreement with previous results showing that *E. coli* cells retain an intact membrane, even when they lose viability upon extended nutrient limitation (Kim *et al*., 2018a). The increased fraction of non-viable cells was still apparent in the early lag phase but largely disappeared in exponential and transition phase due to proliferation of viable cells (Fig. 2A), which was also confirmed by strong dilution

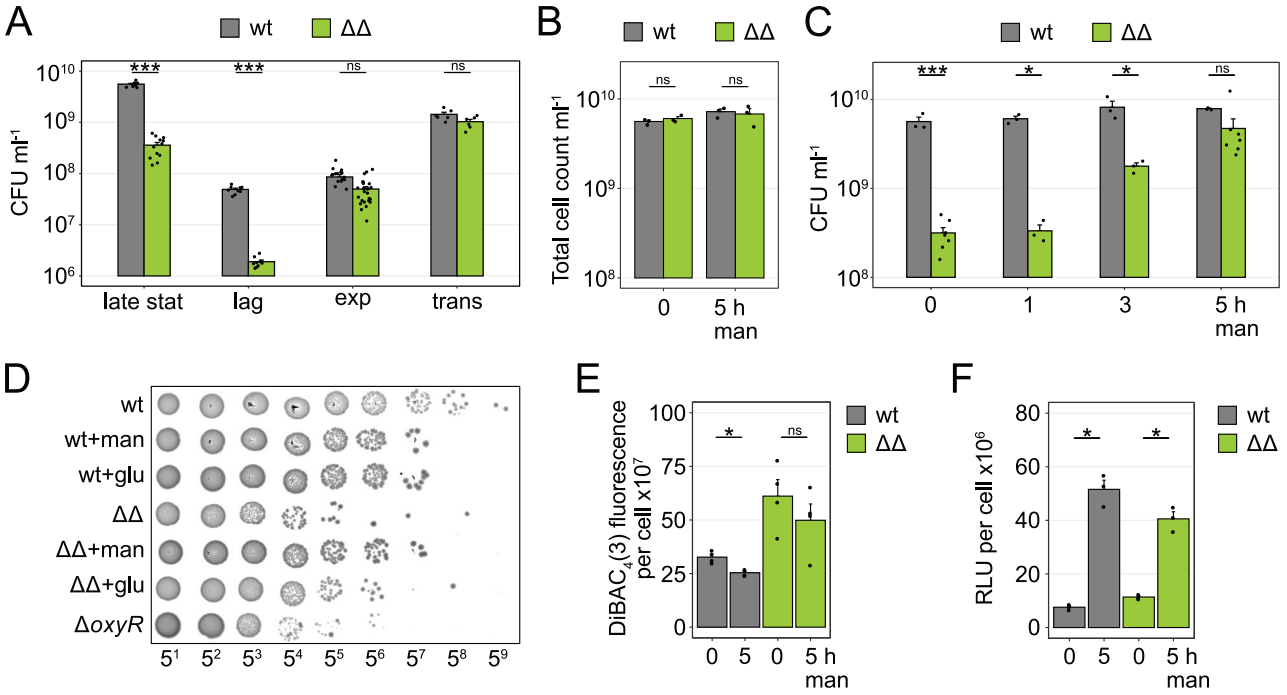

Fig. 2. Viability of mutant Δ1-41 Δ*istR* is reduced in late stationary phase. Cultures of wild-type MG1655 (wt) or Δ1-41 Δ*istR* (ΔΔ) were analysed at different growth stages. Liquid cultures were treated with 10 mM mannitol (man) for the indicated time periods before late stationary phase was reached (20 h after inoculation). Bars represent the mean (±SEM) and black points indicate results of individual biological experiments. A. Viable cell counts were determined at different growth stages (late stat: late stationary phase, 20 h after inoculation; lag: 30 min after 100-fold dilution into fresh medium; exp: exponential phase, OD_{600} of 0.4; trans: transition phase, OD_{600} of 2.0; $n \geq 6$). B. Total cell counts of late stationary-phase cultures were determined by microscopy using a counting chamber ($n = 3$). C. Serial dilutions of cultures at late stationary phase were plated on LB agar to determine viable cell counts ($n \geq 3$). D. Cultures were treated with 10 mM mannitol (man) or 10 mM glucose (glu) for 5 h before late stationary phase was reached. Serial dilutions (as indicated at the bottom) were spotted on LB agar plates. A full scan can be found in Supporting Information Fig. S8. E. Cellular depolarization of late stationary-phase cultures was determined by staining with the potential-sensitive probe $DiBAC_4(3)$. Fluorescence values were normalized to total cell counts ($n = 3$). F. Cellular ATP levels were determined in late stationary phase using luminescence assays. Relative light units (RLU) were normalized to total cell counts ($n = 3$). If applicable, pairwise *t*-tests were performed (***$P < 0.001$, *$P < 0.05$, ns: not significant).

and extended incubation of late stationary-phase cultures (Supporting Information Fig. S9).

We assumed that reduced viability was caused by TisB expression during late stationary phase and impaired membrane functioning due to TisB-dependent depolarization of the inner membrane (Gurnev *et al*., 2012; Berghoff *et al*., 2017). It is known that membranes can be repolarized by metabolic stimuli, e.g. addition of mannitol (Allison *et al*., 2011; Verstraeten *et al*., 2015). Therefore, we tested whether viability was restored by adding mannitol to late stationary-phase cultures. While the wild type was not affected by mannitol, colony counts of the ΔΔ mutant on LB agar plates transiently increased upon prolonged duration of the mannitol treatment. When liquid cultures were treated with mannitol for 5 h before late stationary phase was reached, light scattering patterns in flow cytometry experiments did not change (Supporting Information Fig. S10), but colony counts of the ΔΔ mutant nearly reached wild-type levels (Fig. 2C). Since total cell counts were largely unaffected by mannitol (Fig. 2B), we conclude that mannitol restores viability of the ΔΔ mutant in late stationary phase. In line with this, lag phase of the ΔΔ mutant in liquid cultures was shorter after mannitol treatment (Supporting Information Fig. S11). We tested whether another fermentable sugar, such as glucose, could restore viability of the ΔΔ mutant. Indeed, glucose showed the same positive effect as mannitol when added to liquid cultures before late stationary phase was reached (Fig. 2D). As expected, when late stationary-phase cultures were left untreated and sugars were only added to LB agar plates, viability was not restored (Supporting Information Fig. S8).

We were curious whether mannitol would really affect membrane polarization (Allison *et al*., 2011), and applied the potential-sensitive probe $DiBAC_4(3)$. Since $DiBAC_4(3)$ only enters cells with a depolarized membrane, high cellular $DiBAC_4(3)$ fluorescence indicates strong depolarization. As expected, the ΔΔ mutant had a higher cellular $DiBAC_4(3)$ fluorescence than the wild type in late stationary phase, indicating TisB-dependent depolarization. However, the addition of mannitol did not significantly decrease $DiBAC_4(3)$ fluorescence (Fig. 2E). By

contrast, the addition of mannitol significantly increased cellular ATP levels in both wild-type and ΔΔ cultures (Fig. 2F). Even though mannitol restored viability, it did not increase persister levels of the ΔΔ mutant in late stationary phase (Supporting Information Fig. S4B), suggesting that depolarization alone is not sufficient to trigger persistence in ΔΔ cultures. Further experiments are clearly needed to understand the nature of the reduced viability and its connection to persistence.

The high persistence phenotype of the deregulated mutant depends on tisB *expression*

Our data strongly indicate that post-transcriptional deregulation of the *tisB* gene generates multiple phenotypes related to growth and persistence. To validate that these phenotypes really depend on *tisB* expression, and are not due to secondary mutations or polar effects in the ΔΔ mutant, we specifically impeded *tisB* expression by two different strategies: strong constitutive overexpression of antitoxin IstR-1 from a plasmid (strain ΔΔ pIstR-1) and deletion of the 90-bp *tisB* coding sequence (strain ΔΔΔ*tisB*). Both strains lost the *hip* phenotype in exponential phase (Fig. 3A), but regained culturability in late stationary phase (Fig. 3B), clearly showing that *tisB* expression was responsible for the observed phenotypes.

The lack of regulatory RNA elements in the deregulated mutant enables SOS-independent persistence due to the accumulation of TisB

Transcription of the *tisB* gene is induced upon self-cleavage of the LexA repressor under DNA-damaging conditions (Little, 1991). The *lexA3* mutation generates the non-cleavable LexA3 variant (Fernandez De Henestrosa *et al*., 2000), and avoids induction of the SOS response. Upon CF treatment during exponential phase, induction of *tisB* clearly depends on LexA (Supporting Information Fig. S12A). In exponential phase, wild-type persister levels severely declined due to the *lexA3* mutation (Fig. 4A), confirming previous results (Dörr *et al*., 2009; Völzing and Brynildsen, 2015; Mok and Brynildsen, 2018). By contrast, the *hip* phenotype of the ΔΔ mutant was not affected by the *lexA3* mutation (Fig. 4A), which indicates that persisters in the ΔΔ mutant are generated in a LexA-independent manner before CF is administered.

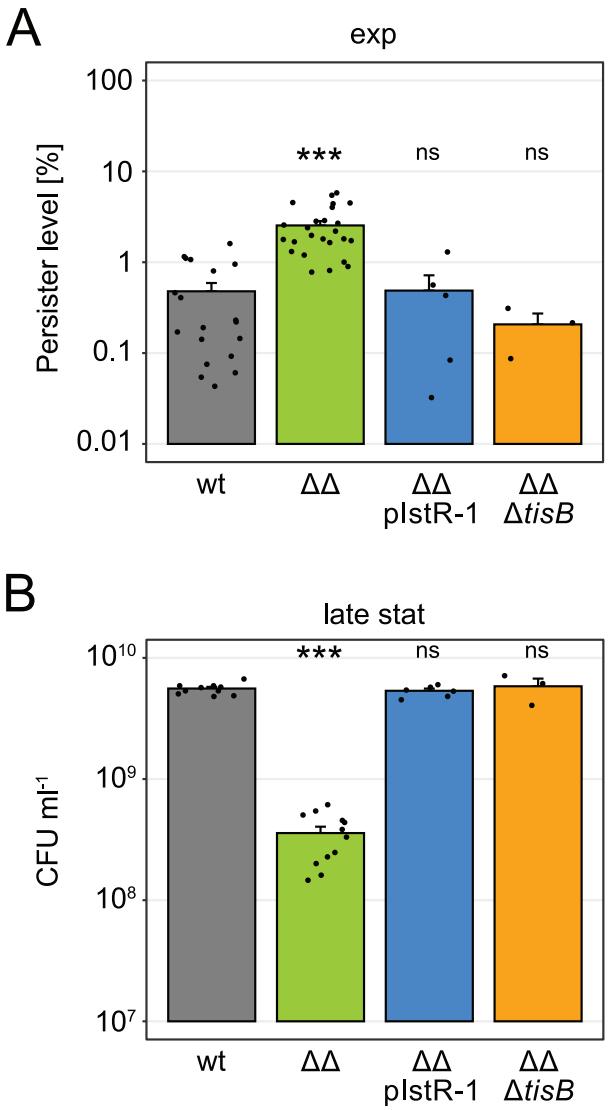

Fig. 3. Phenotypes of mutant Δ1-41 Δ*istR* depend on *tisB* expression.Cultures of wild-type MG1655 (wt), Δ1-41 Δ*istR* (ΔΔ), ΔΔ with IstR-1 overexpression plasmid (ΔΔ pIstR-1) and ΔΔ with deletion of *tisB* (ΔΔΔ*tisB*) were analysed. Bars represent the mean (±SEM; $n \geq 3$). Black points indicate the results of individual biological experiments. A. Late stationary-phase cultures (20 h after inoculation) were diluted 1:100 into fresh medium and grown to exponential phase (exp, OD_{600} of 0.4). Colony counts were determined before and after 6 h of CF treatment (1 μg ml^{-1}; 100× MIC) to calculate persister levels. B. Viable cell counts were determined by plating dilutions of late stationary-phase cultures (20 h after inoculation). Pairwise *t*-tests were performed in comparison to wt (***$P < 0.001$, ns: not significant).

Our physiological data suggest that, in the ΔΔ mutant, toxin TisB accumulates during late stationary phase independent of LexA regulation. Indeed, we detected accumulation of *tisB* +42 mRNA and 3xFLAG-tagged TisB protein in the ΔΔ mutant during late stationary phase (Fig. 4B). Transcriptional regulation of *tisB* was not accountable for the observed accumulation, since (i) *tisB* +1 mRNA did not accumulate in wild-type cultures, (ii) accumulation of *tisB* +42 mRNA in ΔΔ cultures was not affected by the *lexA3* mutation (Fig. 4B) and (iii) a fluorescent fusion to the *tisB* promoter did not reveal an increased promoter activity (Supporting Information Fig. S12B). 3xFLAG-TisB was also detected in ΔΔ cultures during exponential phase, even though

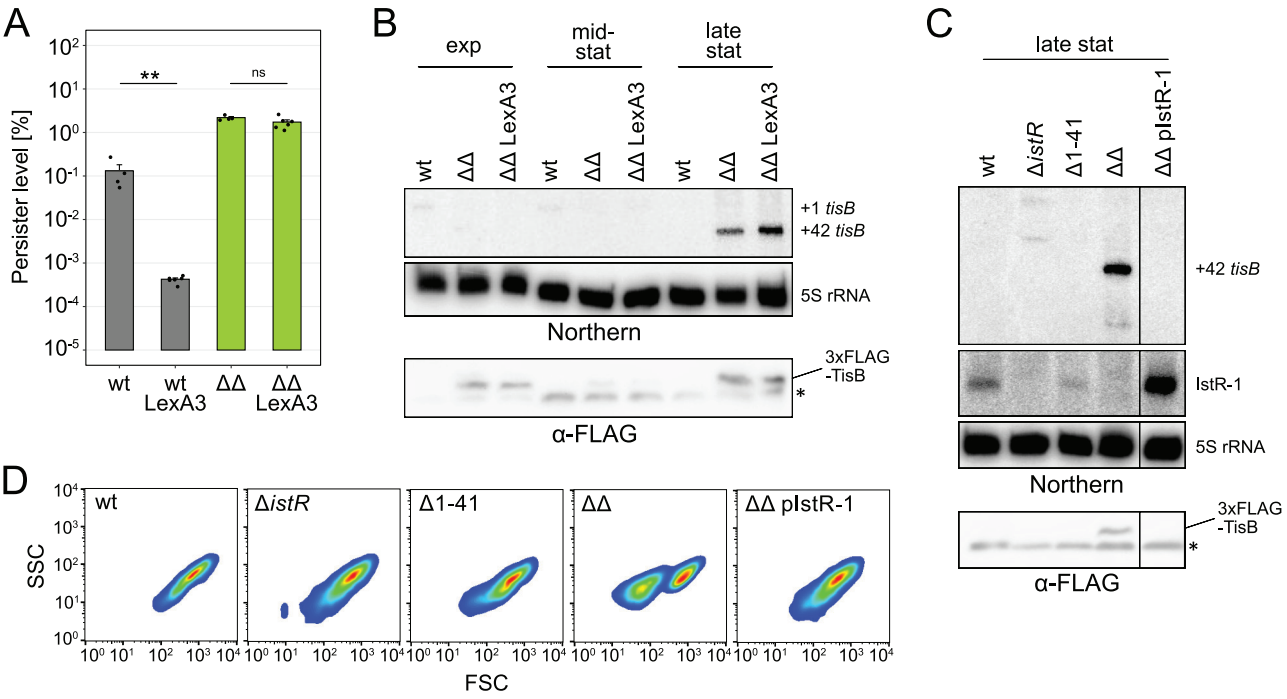

Fig. 4. Deregulation of *tisB* promotes SOS-independent TisB expression. A. Persister levels during exponential phase (OD_{600} of 0.4) after 6 h of CF treatment (1 μg ml^{-1}; 100× MIC). Stationary-phase cultures (16 h after inoculation) were diluted 1:100 into fresh LB medium to obtain exponential-phase cultures. Bars represent the mean (±SEM; $n \geq 4$). Black points indicate the results of individual biological experiments. A pairwise *t*-test was performed (**$P < 0.01$, ns: not significant). B. Northern blot analysis of *tisB* mRNA and immunodetection of 3xFLAG-TisB at different growth stages. Samples were collected at exponential phase (exp, OD_{600} of 0.4), mid-stationary phase (mid-stat, OD_{600} of 4.0) and late stationary phase (late stat, 20 h after inoculation). Specific *tisB* mRNAs (+1 and +42) are indicated. 5S rRNA was probed as loading control. For immunodetection of TisB, only strains with chromosomally encoded 3xFLAG-TisB were subjected to Tricine–SDS-PAGE. 3xFLAG-TisB was detected using an anti-FLAG antibody. The asterisk indicates an unspecific band at approximately 10 kDa that serves as loading control for each growth condition. C. Northern blot analysis of *tisB* mRNA and antitoxin IstR-1, and immunodetection of 3xFLAG-TisB during late stationary phase (late stat, 20 h after inoculation). See (B) for explanation. For illustration purposes, one lane was omitted from the blots (indicated by a vertical line). D. Flow cytometry analysis during exponential phase (OD_{600} of 0.4). Events were depicted as heat maps in scatter plots (FSC: forward scatter; SSC: side scatter). A representative experiment of biological triplicates is shown. (wt: wild type MG1655; ΔΔ: Δ1-41 Δ*istR*; pIstR-1: IstR-1 overexpression plasmid).

tisB +42 mRNA levels were not increased (Fig. 4B). Control experiments showed that the *3xFLAG* sequence itself had no major influence on +42 mRNA levels (Supporting Information Fig. S12C), and that the 3xFLAG-TisB protein detected in exponential phase was not simply a carryover from stationary phase (Supporting Information Fig. S12D). We suggest that constitutive expression of 3xFLAG-TisB in exponential phase is due to basal transcription of *tisB*, but we cannot exclude effects of the 3xFLAG on translation or protein stability.

We speculated that accumulation of 3xFLAG-TisB was due to the lack of post-transcriptional control by antitoxin IstR-1. Indeed, when IstR-1 was present (mutant Δ1-41 or mutant ΔΔ with ectopic IstR-1 expression), neither *tisB* +42 mRNA nor 3xFLAG-TisB protein accumulated in late stationary phase (Fig. 4C). Accordingly, the distinct subpopulation was not observable during outgrowth experiments in strains that had a chromosomal *istR-1* copy or ectopically expressed IstR-1 (Fig. 4D). Since *tisB* +42 mRNA was quite stable (half-life of ∼35 min) in the ΔΔ mutant during late stationary phase (Supporting Information Fig. S13), the lack of IstR-1 probably stabilizes the +42 mRNA and allows its accumulation in stationary-phase cells when turnover of mRNAs is generally low (Barnett *et al*., 2007). This assumption is supported by half-life measurements for the small RNA RybB. In early stationary phase, RybB has a half-life of approximately 8 min (Vogel, 2003). By contrast, in late stationary phase, the half-life of RybB was more than 40 min (Supporting Information Fig. S13).

Conclusions

To date, only few *hip* phenotypes have been characterized in detail (Kaldalu *et al*., 2020). In case of the ΔΔ mutant, it was hypothesized that the *hip* phenotype is caused by stochastic DNA damage and activation of the SOS response, which would enable TisB production due to the lack of post-transcriptional repression (Pennington

and Rosenberg, 2007; Berghoff *et al*., 2017; Berghoff and Wagner, 2019). Here, we show that the *hip* phenotype does not depend on SOS induction, and we also exclude other possibilities concerning transcriptional activation. We rather suggest that post-transcriptional deregulation of the *tisB* gene promotes TisB production during late stationary phase (when the translationally active *tisB* mRNA accumulates due to low RNA turnover) and during exponential phase (when only basal levels of translationally active *tisB* mRNA are present, but translation rate is high).

Our data suggest that TisB production in exponential phase is not sufficient to generate the *hip* phenotype of the ΔΔ mutant. Instead, we observed that TisB production generates a subpopulation of stationary-phase cells, which exhibit a delayed growth resumption (as shown by single-cell lag times), and that this subpopulation is responsible for the occurrence of a high persister fraction in the ΔΔ mutant. TisB-dependent persister formation in wild-type cultures has been denoted drug-induced persistence (Balaban *et al*., 2019), since the drug itself (i.e. a DNA-damaging antibiotic) triggers TisB production and subsequent persister formation (Dörr *et al*., 2010). Persister cells in the ΔΔ mutant match the criteria for stationary-phase (type I) persisters (Balaban *et al*., 2004), since (i) they represent a pre-existing subpopulation of cells, (ii) the number of inoculated cells is proportional to the number of persister cells and (iii) they resume growth with an extended lag phase. Using metabolic labeling and mass spectrometry analysis, we have observed recently that ampicillin-enriched persisters from ΔΔ cultures show enhanced synthesis of RpoS and several RpoS-dependent proteins with functions during stationary phase (Spanka *et al*., 2019). These findings further underscore the notion that TisB persisters in ΔΔ cultures originate from stationary phase.

Type I persistence has also been denoted ‘persistence by lag’, since the prolonged lag phase is a hallmark of this persistence type (Brauner *et al*., 2016). In theory, every event that increases the likelihood of single cells to adopt a prolonged growth-deficient state favours persistence by lag, which has, e.g. been observed upon diauxic shifts (Kotte *et al*., 2014). When bacterial cultures are subjected to cyclic antibiotic treatments, persistence by lag might evolve due to mutations (Fridman *et al*., 2014). In the ΔΔ mutant, persistence by lag occurs due to post-transcriptional deregulation of a type I toxin gene and presumably elevated toxin levels (Rotem *et al*., 2010; Berghoff *et al*., 2017).

We note that persister levels in ΔΔ cultures are surprisingly low at late stationary phase. The reduced viability of ΔΔ cells cannot account for this observation, because mannitol increases viability but does not restore high persister levels. The *tisB* +42 mRNA still accumulated in the presence of mannitol (Supporting Information Fig. S12E), and mannitol was not able to repolarize the membrane of ΔΔ cells. We conclude that mannitol can neither avoid TisB accumulation nor reverse TisB-dependent depolarization. The mannitol-dependent increase in cellular ATP levels rather points to the possibility that mannitol, and probably other sugars like glucose, enter glycolysis and support fermentative processes to restore ATP levels by substrate-level phosphorylation. Hypothetically, elevated ATP levels maintain viable functions but avoid persister formation.

In the current study, we provide a thorough phenotypic characterization of the ΔΔ mutant, which helps to appreciate its *hip* phenotype, and even though the high persister fraction in the ΔΔ mutant might not reflect the wild-type situation, it provides a framework to study TisB-dependent persistence. Importantly, the *hip* phenotype of the ΔΔ mutant is not based on an impaired toxin variant, as in the case of HipA7 (Korch *et al*., 2003; Semanjski *et al*., 2018), but rather on increased expression of a wild-type toxin.

Finally, our data help to explain why type I toxins are tightly regulated by RNA elements. If these regulatory elements are absent, cells might inadvertently enter a deep state of toxin-induced dormancy, from which it is difficult to recover. It is generally assumed that strains with an extended lag phase or *hip* phenotype have a fitness cost due to their impaired growth (Fridman *et al*., 2014; Stepanyan *et al*., 2015). However, depending on the frequency and duration of stressful events, they might outcompete wild-type strains due to their increased stress tolerance, but this advantage would certainly represent a trade-off, and fitness costs might exceed impaired growth. It can be expected that the ΔΔ mutant would suffer from oxidative stress (Edelmann and Berghoff, 2019), membrane perturbations and possibly other disruptive effects due to elevated toxin levels. These fitness costs have likely favoured tight control of type I toxins, which is typically achieved by regulatory RNA elements in wild-type strains (Berghoff and Wagner, 2017).

Acknowledgements

We thank Alisa Rizvanovic, Cédric Romilly and Gerhart Wagner (Uppsala University) for providing strains. We are grateful to Elena Evguenieva-Hackenberg (University of Giessen) for critical reading of the manuscript. We thank Gerrit Eichner (University of Giessen) for helpful comments regarding statistical analysis. We are grateful to John Hook (University of Giessen) for assistance with microscopy. This research was funded by the German Research Council (DFG) in the framework of the SPP 2002 (BE 5210/3-1 to B.A.B.). Work at the Schäberle labs was funded by the Hessen State Ministry for Higher Education, Research and the Arts through the LOEWE program. Open Access funding enabled and organized by ProjektDEAL.

References

Ackermann, M. (2015) A functional perspective on phenotypic heterogeneity in microorganisms. *Nat Rev Microbiol* **13**: 497–508.

Allison, K.R., Brynildsen, M.P., and Collins, J.J. (2011) Metabolite-enabled eradication of bacterial persisters by aminoglycosides. *Nature* **473**: 216–220.

Balaban, N.Q., Helaine, S., Lewis, K., Ackermann, M., Aldridge, B., Andersson, D.I., *et al*. (2019) Definitions and guidelines for research on antibiotic persistence. *Nat Rev Microbiol* **17**: 441–448.

Balaban, N.Q., Merrin, J., Chait, R., Kowalik, L., and Leibler, S. (2004) Bacterial persistence as a phenotypic switch. *Science* **305**: 1622–1625.

Barnett, T.C., Bugrysheva, J.V., and Scott, J.R. (2007) Role of mRNA stability in growth phase regulation of gene expression in the group A *Streptococcus*. *J Bacteriol* **189**: 1866–1873.

Berghoff, B.A., Hoekzema, M., Aulbach, L., and Wagner, E. G.H. (2017) Two regulatory RNA elements affect TisB-dependent depolarization and persister formation. *Mol Microbiol* **103**: 1020–1033.

Berghoff, B.A., and Wagner, E.G.H. (2017) RNA-based regulation in type I toxin–antitoxin systems and its implication for bacterial persistence. *Curr Genet* **63**: 1011–1016.

Berghoff, B.A., and Wagner, E.G.H. (2019) Persister formation driven by TisB-dependent membrane depolarization. In *Persister Cells and Infectious Disease*. Lewis, K. (ed). Cham: Springer International Publishing, pp. 77–97.

Bigger, J.W. (1944) Treatment of staphylococcal infections with penicillin by intermittent sterilisation. *Lancet* **244**: 497–500.

Black, D.S., Irwin, B., and Moyed, H.S. (1994) Autoregulation of *hip*, an operon that affects lethality due to inhibition of peptidoglycan or DNA synthesis. *J Bacteriol* **176**: 4081–4091.

Black, D.S., Kelly, A.J., Mardis, M.J., and Moyed, H.S. (1991) Structure and organization of *hip*, an operon that affects lethality due to inhibition of peptidoglycan or DNA synthesis. *J Bacteriol* **173**: 5732–5739.

Brauner, A., Fridman, O., Gefen, O., and Balaban, N.Q. (2016) Distinguishing between resistance, tolerance and persistence to antibiotic treatment. *Nat Rev Microbiol* **14**: 320–330.

Darfeuille, F., Unoson, C., Vogel, J., and Wagner, E.G.H. (2007) An antisense RNA inhibits translation by competing with standby ribosomes. *Mol Cell* **26**: 381–392.

Dörr, T., Lewis, K., and Vulic, M. (2009) SOS response induces persistence to fluoroquinolones in *Escherichia coli*. *PLoS Genet* **5**: e1000760.

Dörr, T., Vulic, M., and Lewis, K. (2010) Ciprofloxacin causes persister formation by inducing the TisB toxin in *Escherichia coli*. *PLoS Biol* **8**: e1000317.

Edelmann, D., and Berghoff, B.A. (2019) Type I toxin-dependent generation of superoxide affects the persister life cycle of *Escherichia coli*. *Sci Rep* **9**: 14256.

Fernandez De Henestrosa, A.R., Ogi, T., Aoyagi, S., Chafin, D., Hayes, J.J., Ohmori, H., and Woodgate, R. (2000) Identification of additional genes belonging to the LexA regulon in *Escherichia coli*. *Mol Microbiol* **35**: 1560–1572.

Fridman, O., Goldberg, A., Ronin, I., Shoresh, N., and Balaban, N.Q. (2014) Optimization of lag time underlies antibiotic tolerance in evolved bacterial populations. *Nature* **513**: 418–421.

Goormaghtigh, F., Fraikin, N., Putrinš, M., Hallaert, T., Hauryliuk, V., Garcia-Pino, A., *et al*. (2018) Reassessing the role of type II toxin-antitoxin systems in formation of *Escherichia coli* type II persister cells. *MBio* **9**: e00640-18.

Gurnev, P.A., Ortenberg, R., Dörr, T., Lewis, K., and Bezrukov, S.M. (2012) Persister-promoting bacterial toxin TisB produces anion-selective pores in planar lipid bilayers. *FEBS Lett* **586**: 2529–2534.

Harms, A., Fino, C., Sørensen, M.A., Semsey, S., and Gerdes, K. (2017) Prophages and growth dynamics confound experimental results with antibiotic-tolerant persister cells. *MBio* **8**: e01964-17.

Harms, A., Maisonneuve, E., and Gerdes, K. (2016) Mechanisms of bacterial persistence during stress and antibiotic exposure. *Science* **354**: aaf4268.

Helaine, S., Cheverton, A.M., Watson, K.G., Faure, L.M., Matthews, S.A., and Holden, D.W. (2014) Internalization of *Salmonella* by macrophages induces formation of non-replicating persisters. *Science* **343**: 204–208.

Hobby, G.L., Meyer, K., and Chaffee, E. (1942) Observations on the mechanism of action of Penicillin. *Proc Soc Exp Biol Med* **50**: 281–285.

Jõers, A., Kaldalu, N., and Tenson, T. (2010) The frequency of persisters in *Escherichia coli* reflects the kinetics of awakening from dormancy. *J Bacteriol* **192**: 3379–3384.

Kaldalu, N., Hauryliuk, V., Turnbull, K.J., La Mensa, A., Putrinš, M., and Tenson, T. (2020) *In vitro* studies of persister cells. *Microbiol Mol Biol Rev* **84**: e00070-20.

Keren, I., Kaldalu, N., Spoering, A., Wang, Y., and Lewis, K. (2004) Persister cells and tolerance to antimicrobials. *FEMS Microbiol Lett* **230**: 13–18.

Kim, J., Yamasaki, R., Song, S., Zhang, W., and Wood, T.K. (2018b) Single cell observations show persister cells wake based on ribosome content. *Environ Microbiol* **20**: 2085–2098.

Kim, J.-S., Chowdhury, N., Yamasaki, R., and Wood, T.K. (2018a) Viable but non-culturable and persistence describe the same bacterial stress state. *Environ Microbiol* **20**: 2038–2048.

Kim, J.-S., and Wood, T.K. (2016) Persistent persister misperceptions. *Front Microbiol* **7**: 2134.

Korch, S.B., Henderson, T.A., and Hill, T.M. (2003) Characterization of the *hipA7* allele of *Escherichia coli* and evidence that high persistence is governed by (p)ppGpp synthesis. *Mol Microbiol* **50**: 1199–1213.

Kotte, O., Volkmer, B., Radzikowski, J.L., and Heinemann, M. (2014) Phenotypic bistability in *Escherichia coli's* central carbon metabolism. *Mol Syst Biol* **10**: 736.

Kussell, E., and Leibler, S. (2005) Phenotypic diversity, population growth, and information in fluctuating environments. *Science* **309**: 2075–2078.

Kwan, B.W., Valenta, J.A., Benedik, M.J., and Wood, T.K. (2013) Arrested protein synthesis increases persister-like cell formation. *Antimicrob Agents Chemother* **57**: 1468–1473.

Lewis, K. (2010) Persister cells. *Annu Rev Microbiol* **64**: 357–372.

Little, J.W. (1991) Mechanism of specific LexA cleavage: autodigestion and the role of RecA coprotease. *Biochimie* **73**: 411–422.

Masachis, S., and Darfeuille, F. (2018) Type I toxin-antitoxin systems: regulating toxin expression via Shine-Dalgarno sequence sequestration and small RNA binding. In *Microbiol Spectr*: **6**(4). https://dx.doi.org/10.1128/microbiolspec.RWR-0030-2018.

Mok, W.W.K., and Brynildsen, M.P. (2018) Timing of DNA damage responses impacts persistence to fluoroquinolones. *Proc Natl Acad Sci U S A* **115**: E6301–E6309.

Mok, W.W.K., Park, J.O., Rabinowitz, J.D., and Brynildsen, M.P. (2015) RNA futile cycling in model persisters derived from MazF accumulation. *MBio* **6**: e01588-15.

Moyed, H.S., and Bertrand, K.P. (1983) *hipA*, a newly recognized gene of *Escherichia coli* K-12 that affects frequency of persistence after inhibition of murein synthesis. *J Bacteriol* **155**: 768–775.

Nyström, T. (2004) Stationary-phase physiology. *Annu Rev Microbiol* **58**: 161–181.

Pennington, J.M., and Rosenberg, S.M. (2007) Spontaneous DNA breakage in single living *Escherichia coli* cells. *Nat Genet* **39**: 797–802.

Pontes, M.H., and Groisman, E.A. (2019) Slow growth determines nonheritable antibiotic resistance in *Salmonella enterica*. *Sci Signal* **12**: eaax3938.

Rotem, E., Loinger, A., Ronin, I., Levin-Reisman, I., Gabay, C., Shoresh, N., *et al*. (2010) Regulation of phenotypic variability by a threshold-based mechanism underlies bacterial persistence. *Proc Natl Acad Sci U S A* **107**: 12541–12546.

Semanjski, M., Germain, E., Bratl, K., Kiessling, A., Gerdes, K., and Macek, B. (2018) The kinases HipA and HipA7 phosphorylate different substrate pools in *Escherichia coli* to promote multidrug tolerance. *Sci Signal* **11**: eaat5750.

Shi, M., Wan, F., Mao, Y., and Gao, H. (2015) Unraveling the mechanism for the viability deficiency of *Shewanella oneidensis oxyR* null mutant. *J Bacteriol* **197**: 2179–2189.

Song, S., and Wood, T.K. (2020) ppGpp ribosome dimerization model for bacterial persister formation and resuscitation. *Biochem Biophys Res Commun* **523**: 281–286.

Spanka, D.-T., Konzer, A., Edelmann, D., and Berghoff, B.A. (2019) High-throughput proteomics identifies proteins with importance to postantibiotic recovery in depolarized persister cells. *Front Microbiol* **10**: 378.

Stepanyan, K., Wenseleers, T., Duéñez-Guzmán, E.A., Muratori, F., Van den Bergh, B., Verstraeten, N., *et al*. (2015) Fitness trade-offs explain low levels of persister cells in the opportunistic pathogen *Pseudomonas aeruginosa*. *Mol Ecol* **24**: 1572–1583.

Unoson, C., and Wagner, E.G.H. (2008) A small SOS-induced toxin is targeted against the inner membrane in *Escherichia coli*. *Mol Microbiol* **70**: 258–270.

Van den Bergh, B., Fauvart, M., and Michiels, J. (2017) Formation, physiology, ecology, evolution and clinical importance of bacterial persisters. *FEMS Microbiol Rev* **41**: 219–251.

Veening, J.-W., Smits, W.K., and Kuipers, O.P. (2008) Bistability, epigenetics, and bet-hedging in bacteria. *Annu Rev Microbiol* **62**: 193–210.

Verstraeten, N., Knapen, W.J., Kint, C.I., Liebens, V., Van den Bergh, B., Dewachter, L., *et al*. (2015) Obg and membrane depolarization are part of a microbial bet-hedging strategy that leads to antibiotic tolerance. *Mol Cell* **59**: 9–21.

Vogel, J. (2003) RNomics in *Escherichia coli* detects new sRNA species and indicates parallel transcriptional output in bacteria. *Nucleic Acids Res* **31**: 6435–6443.

Vogel, J., Argaman, L., Wagner, E.G.H., and Altuvia, S. (2004) The small RNA IstR inhibits synthesis of an SOS-induced toxic peptide. *Curr Biol* **14**: 2271–2276.

Völzing, K.G., and Brynildsen, M.P. (2015) Stationary-phase persisters to ofloxacin sustain DNA damage and require repair systems only during recovery. *MBio* **6**: e00731-15.

Wilmaerts, D., Bayoumi, M., Dewachter, L., Knapen, W., Mika, J.T., Hofkens, J., *et al*. (2018) The persistence-inducing toxin HokB forms dynamic pores that cause ATP leakage. *MBio* **9**: e00744–e00718.

Supporting Information

Additional Supporting Information may be found in the online version of this article at the publisher's web-site:

Fig. S1. Total cell counts during lag phase.
Fig. S2. Single-cell lag time determination.
Fig. S3. Length distribution of wt and ΔΔ cells during late stationary and exponential phase.
Fig. S4. Persister levels at different growth stages.
Fig. S5. Verification of persister assay parameters.
Fig. S6. The size of subpopulation A is affected by dilution of pre-cultures.
Fig. S7. Live-dead cell viability assay.
Fig. S8. Analysis of viability using spot assays.
Fig. S9. Viable cell counts during exponential phase.
Fig. S10. Flow cytometry analysis of late stationary-phase cultures with mannitol.
Fig. S11. Mannitol counteracts the prolonged lag phase of the ΔΔ mutant.
Fig. S12. Expression levels of *tisB* under various conditions.
Fig. S13. Half-life determination of *tisB* +42 mRNA at late stationary phase.
Table S1. Strains and plasmids used in this study.
Table S2. Oligodeoxyribonucleotides used in this study.